



Universidad Autónoma
de Madrid

Biblos-e Archivo
Repositorio Institucional UAM

Repositorio Institucional de la Universidad Autónoma de Madrid

<https://repositorio.uam.es>

Esta es la **versión de autor** del artículo publicado en:
This is an **author produced version** of a paper published in:

Advanced Functional Materials 26.41 (2016): 7394-7405

DOI: <https://doi.org/10.1002/adfm.201603103>

Copyright: © 2016 WILEY-VCH Verlag GmbH & Co. KGaA, Weinheim

El acceso a la versión del editor puede requerir la suscripción del recurso
Access to the published version may require subscription

DOI: 10.1002/ ((please add manuscript number))

Full Paper

Clay-graphene nanoplatelets functional **conducting** composites

Eduardo Ruiz-Hitzky, Maria Madalena C. Sobral, Almudena Gómez-Avilés, Claudia Nunes, Cristina Ruiz-García, Paula Ferreira, Pilar Aranda*

Prof. E. Ruiz-Hitzky, Dr. A. Gómez-Avilés, Dr. P. Aranda
Materials Science Institute of Madrid, CSIC, c/Sor Juana Inés de la Cruz 3, Cantoblanco,
28049 Madrid, Spain.

E-mail: eduardo@icmm.csic.es

MSc. M. M. C. Sobral, Dr. C. Nunes, Dr. P. Ferreira
CICECO - Aveiro Institute of Materials, Department of Materials and Ceramic Engineering,
University of Aveiro, 3810-193 Aveiro, Portugal

MSc. C. Ruiz-García
Chemical Engineering Section, Faculty of Sciences, UAM, Cantoblanco, 28049 Madrid,
Spain

Keywords: clay, graphene, graphite, composite, biopolymer

An approach to functionalize graphene-based materials has been developed by assembling graphene nanoplatelets (GNP) with clay minerals. Under convenient sonomechanical treatment, clay-GNP mixtures may produce very stable water dispersions in particular using sepiolite fibrous clay. While in absence of clay a rapid decantation of GNP in water is observed, in the presence of sepiolite the resulting dispersions remain stable during months without syneresis effects. Rigid, but flexible self-supported films, are easily obtained by filtering of these dispersions. As the electrical percolation threshold corresponds to sepiolite/GNP composites of 0.5:1 in weight, doping these systems with MWCNTs significantly enhances their electrical conductivity. The particular microporosity of the sepiolite component allows interactions with molecules, such as organic dyes, as well as polymers, such as biopolymers, opening the way to functional materials for advanced applications due to their inherent conductivity afforded by the GNP and MWCNTs carbonaceous components. In fact, using very small amount of MWCNT together with GNP

can be obtained composites with significant electrical conductivity, maintaining the enhanced mechanical properties, at a lower cost.

1. Introduction

Graphite and most clay minerals are structurally organized as 2D solids representing an abundant natural resource used during centuries for relevant quotidian applications. Graphite has acquired a particular interest in the past ten years since the discovery by Geim and Novoselov, reporting its mechanical exfoliation into graphene (monolayers of carbon).^[1] As it is well known, **graphene and related materials, including diverse 2D solids**, represent nowadays an attractive focus for research and even commercialization of new products, due to their extraordinary properties arisen from their unique structure that give rise to improved applications in critical fields, as for instance production and storage of energy, components of electronic devices, polymer nanocomposites, and advanced coatings development.^[2] However, as occurs with carbon nanotubes (eg. MWCNTs), graphene materials such as reduced graphene oxides (rGO) are too expensive for diverse industrial applications hence naturally occurring graphite, processed as graphene nanoplatelets (GNP), emerges as an interesting alternative to MWCNTs and rGO conducting carbonaceous solids.

On the other hand, clay minerals have been traditionally used in ornamental objects and building materials, such as pottery and ceramic, bricks and tiles, etc., showing also a 2D structural arrangement, based in this case on the stacking of silicate sheets that can be also submitted to delamination.^[3] Graphene is essentially an electrically and thermally conducting material whereas clays, except the group of layered hydrated aluminosilicates that can exhibit ion-conductivity, are basically electrical and thermal insulating solids. However, certain aspects of both types of 2D solids are coincident as they exhibit interesting surface properties, including porosity and intercalation ability, which can be used for the preparation of hybrid, biohybrid and composite materials provided of potential interest in advanced applications.

It is scarcely known that clay-graphite composites have been commonly used since various centuries ago. Actually, they are one of the most used materials because they are employed as an essential component in pencils, i.e. the so-called *graphite leads*. Poor quality pencils were produced using pure graphite powder. The combination of fine fractions of clay minerals and graphite powder consolidated as a composite in a thermal treatment and processed as sticks is the basis for the fabrication of conventional pencil cores, being the procedure patented by N. J. Conté in 1795. These graphite-clay composites (*pencil leads*) encased in wood allowed an efficient use of pencils. The adjustment of the clay: graphite ratio gives a good control of the lightness or darkness of the graphite mark left on the paper.^[4] So, the “tone” of many pencils is graded using a continuum proportion, for instance for Derwent pencils from 53% of clay (9H, the hardest) to 7% of clay (9B, the softest).^[5] In this nomenclature H is used to indicate the hardness and to B the blackness of pencils, the medium corresponding to HB containing ca. 26% of clay (**Figure 1**).

Currently, there are known various procedures for assembling clays and graphite-like components at the nanometric scale. For instance, generation of carbon-clay nanostructured materials by the so-called template carbonization method consists in the introduction of organic compounds, such as monomers or polymers (i.e. polyacrylonitrile, PAN), into the intracrystalline nanospace of clay minerals (i.e. montmorillonite) followed by thermal treatment in absence of oxygen. This procedure was first reported by Kyotani and co-workers,^[6] and, later on, applied by other authors using diverse types of silicates from the clay minerals family.^[7-10] In this case the pyrolysis of PAN previously intercalated in clays gives rise to clay composites containing carbonaceous materials provided with good electrical conductivity. These resulting systems point out to nanostructured materials composed by the silicate backbone assembled to conducting carbon, probably containing graphene-like species.^[8] Although the carbon-clay materials may have interest *per se*, most of the carbon-

1 clay precursors are used as source of nanostructured carbons that show electronic conductivity,
2 being useful for diverse applications such as electrode materials for secondary Li-batteries
3 and supercapacitors.^[10] It should be remarked that the use of carbon-clay composites without
4 removal of the clay substrate may provide these materials with additional advantages as for
5 instance the easy functionalization of the silicate substrate to develop active phases for sensor
6 devices.^[11-13] More recently, layered silicates, such as vermiculite provided of bigger crystals
7 than related clay minerals belonging to the smectite family, have been combined with
8 asphaltene molecules and further thermally transformed on graphene composites showing
9 sheets with 8–10 graphene layers and tens of micrometers width.^[14]

10 We have also recently reported the on-surface graphene production using clays and other
11 porous solids and natural resources such as carbohydrates (i.e. sucrose) or proteins (i.e.
12 gelatin) as carbon precursors. The resulting clay-supported graphene materials show
13 remarkable characteristics such as simultaneous conducting behavior, together with chemical
14 reactivity and adsorption features provided by the silicate backbone, which are of interest for
15 diverse high-performance applications.^[15-16] The procedure consists in the impregnation of the
16 porous solids with the precursors followed by a thermal treatment in absence of oxygen at
17 temperatures below 1000 °C and, interestingly, graphene-like flakes are formed without
18 requiring addition of reducing agents.^[17] Among other porous solids, clay minerals of
19 different topologies, i.e. from layered silicates (e.g. montmorillonite) to fibrous sepiolite, have
20 been used as porous substrates to produce those carbon-composites. In particular, the use of
21 sepiolite may produce additional benefits due to the presence of silanol groups and textural
22 behavior allowing an easy controlled functionalization of resulting composites.^[15,18] Sepiolite
23 and palygorskite are fibrous clays showing relevant properties afforded by their unique
24 morphological and surface features, making these silicates very attractive compared to
25 “conventional clays“, such as montmorillonite and other 2D clay minerals in view to new
26 applications and advanced materials preparations.^[19] The crystalline structure of sepiolite is

related to talc-like ribbons placed parallel to the fiber axis (c-axis) (**Figure 2**), which are built-up by blocks alternating with structural cavities (tunnels) that give rise to a fibrous silicate provided with micro- and meso-porosity, elevated specific surface area and therefore, high adsorption capacity.^[20-22] In clay-carbon composites based on sepiolite and sucrose (table sugar) show the formation of C=C bonds attributable to graphene-like materials are produced, in agreement with XPS and Raman spectra.^[15, 17]

Finally, it should be noted that direct combination of clays and graphene based materials produced in large-scale, such as graphene oxide (GO) or reduced graphene oxide (r-GO) nanoplatelets, dispersed in water appears as an useful way to prepare clay-graphene composites conformed as films with improving characteristics such as superior flexibility, electrical conductivity and flame retardancy. In this way, direct reduction of GO sheets in the presence of exfoliated montmorillonite nanoplatelets is one of the ways applied to develop these water-dispersible composites.^[23] Contrarily to graphene-based materials produced directly from graphite such as GNP, particulated graphene-oxide produced by well-known Hummers method^[24] and related procedures, contains hydroxyls and other chemical functions allowing its easy aqueous dispersion. So, GO gives rise in an easy way to clay-composite dispersions of good stability but requiring elevated clay/GO (w/w) ratio (>10).^[25] Moreover, these systems, even after reduction of GO species, lead to solids provided of lower conductivity than the corresponding materials based on GNP due to the strong effect of the applied reducing procedure.^[26] Clays of different morphology such as halloysite nanotubular clays, have been also assembled to graphene-like compounds to produce hybrid systems as reported by Liu et al..^[27] In view to the incompatibility between both negatively charged 2D particles (halloysite and graphene oxide, GO), these last authors introduced a selective modification of the outmost clay surface by grafting of γ -aminopropyltriethoxy groups that, under acidic conditions, transforms halloysite into a positively charged surface allowing their combination with GO in an electrostatic way.^[27]

In this contribution, we report and discuss on the use of layered clays of the montmorillonite type, as well as fibrous sepiolite, to develop stable dispersions of graphene-like compounds by direct assembling under sonomechanical treatments that facilitates the dispersion and re-stacking of delaminated 2D solids as well as the defibrillation of sepiolite particles. The goal is to demonstrate the ability of certain clay minerals to stabilize water suspensions containing graphite derivatives. Thus, in this work, it is employed commercial graphene nanoplatelets directly produced from natural graphite by industrialized mechanical exfoliation. These GNP are composed of multilayer graphene flakes with an average diameter in the order of 5 μm . Without oxidation and reduction treatments, this product has a well ordered layered crystal structure, elevated carbon content (ca. 99%), and displays high electrical and thermal conductivity among other attractive characteristics recently reported.^[28-31] The resulting clay-graphene systems prepared with these GNP may produce stable water dispersions of great interest for diverse applications, as for instance to obtain conductive paints and flexible self-supported composites provided of electrical conductivity. Also, clay-graphene dispersions can facilitate the preparation of highly homogeneous polymer-clay-graphene composites, which can be conformed as films provided of good mechanical and electrical properties. This last issue is also investigated in the present work.

2. Results and discussion

2.1. Clay/graphene-nanoplatelet composite materials

Graphene nanoplatelets (GNP) consisting in partial exfoliated graphite crystals do not form stable dispersion in water, even after longtime sonomechanical treatments (**Figure 3A**). A first set of experiments trying to develop stable clay-GNP water dispersions was carried out using a layered clay, in this case Na-montmorillonite (CloisiteTM-Na). As it is well known, this type of clay mineral shows a remarkable swelling ability in aqueous media giving rise to stable colloidal systems. However, we have observed that when it was combined with GNP it

does not form dispersions able to remain stable with time (**Figure 3B**). By varying several experimental conditions such as montmorillonite/graphene (w/w) proportion, water content in the system, and total energy applied in the ultrasound irradiation (US), it can be determined the best conditions for obtaining durable clay/GNP dispersions. In this way, fresh prepared dispersions, containing 20 mg of GNP and 10 mL of water with montmorillonite-Na/GNP 2.5:1 (w/w) ratio corresponding to a 28.6% of graphene in the mixture and applying a total US energy of 1 kJ, remain dispersed during a maximum of *ca.* 24 h. Overpassed this time, it is clearly observed a syneresis effect leading finally to a complete decantation of the solids when the elapsed time was superior to 72 h. (Figure 3B). Although the GNP particles appear well integrated within the montmorillonite silicate, as observed in the corresponding FE-SEM images (**Figure 3B**), these clay-graphene nanoplatelets systems offer a limited stability in water dispersions.

In contrast, when montmorillonite is replaced by sepiolite (PangelTM) the resulting dispersions show an excellent stability (**Figure 4**). For identical experimental conditions there are not observed syneresis effects for several weeks or even after months of preparation. Sepiolite-rich dispersions maintain an elevated viscosity even after longtime of preparation. This is for instance the case of 10:1 ratio in sepiolite/GNP composite showing a Brookfield viscosity at room temperature of *ca.* 2000 cP (5 rpm), measured after 6 months of preparation. The extraordinary stability of these sepiolite-GNP suspensions allows an easy preparation of highly homogeneous films by vacuum filtration, operating in the same way than reported for the preparation of *hybrid buckypapers* using sepiolite and MWCNTs.^[32] These clay-carbon composites prepared as films can be related to hybrid membranes resulting from the assembly of GNP and MWCNTs (i.e. in absence of clays), which have been described as materials that improve flame retardancy in reinforced epoxy composites.^[31] The sepiolite-GNP self-supported films here prepared can be easily peeled off from the Millipore membrane used as filter, which were dried overnight at 65 °C, before characterization. These films are flexible

and can be bent without breaking as shown in **Figure 4C**. Additional incorporation of MWCNTs is possible during the mixing process of the clay and GNP in view to improve mechanical and electrical properties (*vide infra*).

Examples of diffractograms corresponding to various self-supported films formed by combination of sepiolite and GNP in diverse proportions, from 9.3% to 62.7% of carbon, are shown in **Figure 5**. The presence of both microcrystalline solids, sepiolite and GNP, are clearly observed in the XRD patterns of the composite films prepared from variable clay/carbon content. The signal of GNP at 0.33 nm corresponds to the typical van der Waals gap-distance between graphene layers. The most intense signal of starting sepiolite observed at *ca.* 12 nm corresponds to the [100] crystallographic plane of this silicate, being detected for those clay/GNP composites with a ratio of components greater than 0.5:1 (w/w). In the equivalent MWCNTs doped materials, the presence of carbon nanotubes is not detected in the XRD patterns due to the low amount incorporated in the corresponding composites. FE-SEM images of sepiolite/GNP films corresponding to samples prepared with different ratio (**Figure 6**) show a good dispersion of GNP within microfibers of sepiolite, remaining well integrated in this silicate (**Figure 1S**). This situation is also visualized in cross-section FE-SEM images that show the trend of GNP layers and clay fibers to become organized in the composite as planar stacking integrating both components (**Figure 6C**). Only for materials with low content in sepiolite it appears some aggregates of GNP (**Figure 6B**). This circumstance indicates that percolation should be attained for systems with high content in GNP in detriment to the better stability afforded by the higher amount of clay mineral, which is confirmed by electrical conductivity measurements (**Table 1**), since only films with higher proportion of GNP (sepiolite/GNP, 0.5:1) have conductivity *through-plane* and *in-plane*. The incorporation of MWCNTs increases the connectivity between conducting particles (**Table 1**), giving rise in the adopted experimental conditions to a remarkable separation of the carbon nanotubes, which usually tend to form bundles. At this respect, it was already reported the ability of

sepiolite and MWCNTs to form “hybrid buckypapers” where the silicate fibers and the carbon nanotubes are intimately assembled, being the resulting films provided of good electrical conductivity.^[32]

A remarkable homogeneity of the clay and carbonaceous component is observed by EDX analysis in the diverse self-supported films based on sepiolite and GNP (**Figure 2S**). For instance, the sepiolite/GNP composite of 5:1 (w/w) composition contains as major components: oxygen (36.8%), silicon (25.4%), carbon (19.8%), magnesium (13.6%) and iron (2.9%) as determined by EDX (**Figure 2S**). The corresponding FE-SEM images show that all these elements are equally distributed among the selected area of sample, indicating the excellent homogeneity of components distribution at least at the micrometer scale at which operates the microscope used.

Diverse characteristics, such as carbon content deduced from elemental chemical analyses, specific surface area and electrical conductivity, of various sepiolite-based films prepared from different initial content of GNP and GNP/MWCNTs are collected in **Table 1**. The carbon content determined from elemental chemical analyses is close to the expected values calculated from the starting carbon-clay mixture, indicating that both components are well integrated in the final product, giving rise to homogeneous materials at least at the macroscopic range. To explain the discrepancy between experimental determinations and the theoretical ratio of clay and carbon components, it should be taken into account that the water physically adsorbed in sepiolite is in equilibrium with the atmospheric humidity and may represent about 10% (w/w), affecting significantly the composite ratio determination.

The FTIR spectra of the sepiolite/GNP composites are similar to those of starting sepiolite indicating the absence of appreciable perturbations of the silicate bands due to its interaction with the GNP and MWCNTs carbonaceous components (**Figure 3S**). Raman spectra of GNP (**Figure 7**), clearly show the presence of typical D and G bands of graphite and graphene-like materials, which appears at 1344 and 1570 cm^{-1} , respectively, as well as the band at *ca.* 2700

cm⁻¹ assigned to G' band (also referred to as 2D band). The spectrum of the sepiolite-GNP composite (doped with MWCNTs), selected as an illustrative example in the **Figure 7**, shows signals centered at the same wavenumbers to that of GNP but showing some differences, besides the spectrum background characteristic of the fluorescent properties of natural sepiolite from Vallecas-Vicálvaro deposits, here used. While the G band does not suffer significant changes, D band intensity increases, which can be related to a major contribution of defects in the graphitic plane. Something similar happens with G' signal, which shows changes both in shape, being more symmetric than in the spectrum of GNP, and position, appearing at lower wavenumbers, which may be to a possible delamination of GNP induced by the ultrasonication process.^[33,34]

The thermal and thermogravimetric analyses (DTA and TGA, respectively) of composites are also quite similar to those of starting individual components, i.e. sepiolite and GNP (**Figure 4S**). The GNP component is very stable towards the temperature in the experimental conditions of measurement (under N₂ flux), whereas sepiolite maintains its characteristic weight losses corresponding to the elimination of water molecules in different environments. For instance, the loss of weight at temperature below 100 °C, assigned to physically adsorbed and zeolitic water molecules, is decreased in the composite from 10.0% to 6.4%, which corresponds to a decrease of 36% not too far from the theoretical one (33.3%, i.e. considering the actual amount of C in the sample).

Among the most significant characteristics of the prepared clay-graphene nanoplatelets composites there are their textural properties mainly afforded by the sepiolite component and the electrical conductivity assured by the GNP solid. The elevated specific surface area and porosity of the starting sepiolite (**Table 2**) is almost maintained in the composites but decreases by a dilution effect upon its mixture with the GNP carbonaceous material, which shows the lowest value of specific surface area for 0.5:1 proportion (**Table 1**). The N₂ adsorption-desorption isotherms of sepiolite and derived materials are represented in **Figure 8**,

which were assigned to the type I/II with hysteresis loops of type H3 according to the IUPAC classification.^[35] In the region of low relative pressure, the isotherm fits with the type I, attributed to a micropore filling process. At higher relative pressure it is observed a multilayer adsorption followed by capillary condensation, owing to the presence of mesoporosity in the structure, which is ascribed to a type II. This type of isotherm is associated with a micro-mesoporous structure with type-H3 hysteresis loop, which is commonly ascribed to materials with slit-shaped pores and plate-like particles.^[35] The graphene-nanoplatelets show an isotherm associated to the type II with a type H3 hysteresis loop, called type IIb by Rouquerol et al..^[35] Type IIb isotherms are usually obtained for solids with aggregates of plate-like particles and non-rigid slit-shaped pores. The textural parameters calculated from these isotherms are summarized in **Table 2**. Sepiolite is well known as a natural microporous silicate provided with a large total pore value (*ca.* 0.6 cm³ g⁻¹) and an elevated specific surface area, as above indicated. These interesting textural characteristics make this silicate of great interest for diverse industrial applications mainly based on its adsorption properties.^[19,21] GNP-150 from KNANO shows very low microporosity being a solid whose porosity can be essentially associated with its external surface. The value of the specific surface area of these graphene-nanoplatelets (41 m²/g) is in the same order than the one published by the supplier.^[36]

The values of electrical conductivity measured in perpendicular direction (through-plane, *TP*) in sepiolite/GNP composites are much lower than the one of starting GNP (*ca.* 80 S m⁻¹) due to the sepiolite insulating capacity (**Table 1**). The lamellar habit of the graphene nanoplatelets makes the predominant disposition of this material parallel to the plane of the particles, being separated by the silicate fibers and therefore decreasing the electrical conductivity in many cases till the limit of detection of the equipment (**Table 1**). However, the in-plane conductivity of the composite films determined by the van der Paw method (*four points probe*

technique) is easily measurable, giving values of conductivity specially elevated for MWCNTs doped materials (**Table 1**).

As it is well known, sepiolite is a microporous silicate that exhibits the interesting ability to adsorb gases, as well as ions and molecules in solution, showing in certain cases specific selectivity imposed by the size and shape of the adsorbate.^[22] These textural characteristics associated with their electrical conductivity can be of great interest for new potential applications of these graphene-clay materials. For instance, the selective molecular adsorption towards organic dyes of the methylene blue (MB) type allows the preparation of colored materials simultaneously provided with electrical conductivity, which is required for developing conductive inks for multiple uses including printed circuit boards. Sepiolite/GNP/MWCNTs self-supported films spontaneously adsorb MB from very dilute aqueous solutions (*ca.* 10^{-5} M) giving rise to blue composites (**Figure 9**). From elemental chemical analyses it has been found an increase of 5.31% in weight of carbon after saturation of sepiolite/GNP/MWCNTs (2:1:0.1) with MB solution, which corresponds to an adsorption of $17 \cdot 10^{-3}$ mol/100 g. This adsorbed amount is in the order of magnitude of that determined in the adsorption isotherm region where monomeric and dimeric species can be adsorbed by sepiolite.^[37] It has been reported that in these conditions, the MB molecules are irreversibly entrapped into the tunnels of sepiolite of nanometer section giving rise to very stable colored materials.^[22] This is the principle of the Maya Blue concept developed several centuries ago and recently interpreted on the basis of physico-chemical characterization,^[38,39] which allows in the preparation of pigments of extraordinary thermal and chemical stability by inclusion of indigo in the structural cavities of palygorskite, an alike clay mineral closely related with sepiolite. The stability of sepiolite-dyes adducts has been nowadays profited to prepare colored polymers and geopolymers.^[40] Although conductive colored sepiolite/GNP/MWCNTs composites could be potentially used as main components in conducting inks (**Figure 5S**), other potential applications may address the development of

new active phase of sensors, electrocatalysts, elements for solar cell devices, or even, in a new concept of OLEDs by inclusion of organic semiconductors in the sepiolite structural cavities.

To check the generalization of the process in the clay-GNP films preparation, it has been also tested graphene-nanoplatelets from other origin/supplier, as it is the case of multilayered graphene named as GP500. This type of graphene-like material contains a smaller amount of graphene layers (5-10 in this case) in comparison with GNP and shows a specific surface area 10 times greater than GNP. Sepiolite-GP500 self-supported films were prepared under identical experimental conditions than those applied for the preparation of clay-GNP materials. These films also show a good homogeneity and flexibility with physical-chemical characteristics quite similar to those of the above reported sepiolite-GNP composites. FE-SEM images (**Figure 6S**) show for instance the uniform distribution of graphene nanoplatelets in the composite, as well as a detail obtained at higher magnification, displaying the intimate coverage of GP500 by the sepiolite fibers in a comparable way to the one observed in GNP composites (**Figure 6SA**). The Raman spectrum of sepiolite/GP500 (2:1 w/w, i.e. with ca. 33% of carbon content) composite, selected as example, is quite similar to that obtained from sepiolite-GNP materials showing the typical D and G bands at 1336 and 1574 cm^{-1} and the G' band at 2692 cm^{-1} (**Figure 7S**).

The electrical conductivity of sepiolite/GP500 or GNP (ca. 33% of carbon w/w) measured in both cases parallel to the film (*in-plane*), are undetectable, but the resulting films of sepiolite/GP500 doped with MWCNTs show conductivity values (data not show) inferior to the sepiolite-GNP equivalent composites, in agreement with the major conductivity of starting GNP compared with GP500 graphene-nanoplatelets (*vide supra*). For instance, the conductivity of sepiolite/GP500/MWCNTs 2.5:1:0.1 (ca. 28% of carbon w/w) films is ca. 24 S m^{-1} whereas the same composite prepared with GNP shows a conductivity of ca. 76 S m^{-1} . By increasing the amount of graphene-nanoplatelets, it is observed an enhancement of

conductivity reaching values of 434 and 2,633 S m⁻¹ for the sepiolite/graphene nanoplatelets/MWCNT 0.5:1:0.1 (62.5% of carbon w/w) with GP500 and GNP, respectively.

2.2. Clay/graphene nanoplatelets polymer composites

Another important issue derived from these conducting materials is the possibility to combine them with polymers in view to prepare conductive composites. Sepiolite has been largely studied as an additive for nanofiller reinforcement of polymer matrices of diverse nature.^[18,19]

The assembly of this silicate with polymers of natural origin (biopolymers) leads to bionanocomposites provided of interesting both mechanical and functional properties.^[19,41-44]

The good stability of water colloidal dispersions of GNP in presence of sepiolite facilitates the further incorporation of polymers able to form hydrogels, such as alginate. In the sepiolite/GNP/MWCNTs systems this polysaccharide was incorporated under ultrasound (US) irradiation as reported in the experimental section with the aim to obtain bionanocomposites provided with electrical conductivity. It has been observed a different stability of the resulting bionanocomposite dispersions depending on the incorporation sequence of the biopolymer with respect to the sonomechanical treatment. Thus, the dispersions are not stable when alginate is added before the ultrasonic treatment observing syneresis effects, with a complete loss of stability after 5 days since the preparation (**Figure 8S**). In these circumstances it can be supposed that a breakage of the alginate chains produced by the ultrasound irradiation take place, decreasing the interaction among them and with sepiolite. Similar effects of the ultrasonication applied to other sepiolite-polysaccharide systems have been previously considered.^[45] On the contrary, very stable dispersions are obtained when the alginate incorporation was carried out after the US application, avoiding syneresis effects after several days of preparation (**Figure 8S**). In these last conditions were also incorporated MWCNTs, with the aim to increase the conductivity in the final systems as it was promoted in the clay/GNP systems (*vide supra*). The corresponding dispersions were

also stable and after casting and drying at controlled temperature and humidity (30°C/ 60% RH) gave rise to self-supported films showing homogeneous aspect when amounts of ca. 10% (w/w) of MWCNTs were incorporated (**Figure 10**). Higher amounts of carbon nanotubes lead to inhomogeneous materials and the corresponding films showed a marked shrinking behavior. FE-SEM images (**Figure 9S**) of sepiolite/GNP/alginate and sepiolite/GNP/MWCNTs/alginate bionanocomposites show a tendency to a flat organization of the components when conformed as films by a casting process as observed in the images corresponding to the surface of the film and to its cross-section, respectively (**Figure 9SA and Figure 9SB**).

The results of mechanical properties measurements carried out in films of diverse sepiolite-GNP-alginate compositions, and the corresponding MWCNT doped systems containing 10% (w/w) of carbon nanotubes with respect to the GNP content, are plotted in **Figure 11**. Apparently there is not a direct correlation between the variation of mechanical properties of the polymer matrix (alginate) by the incorporation of GNP and sepiolite. However, despite of the relatively high standard deviations, it can be observed a tendency to decrease the elongation at break with the increase of GNP and MWCNT contents, whereas the tensile and the Young modulus values are almost maintained. The incorporation of sepiolite decreases the mechanical properties of the starting alginate, except for the results of the elongation at break (sample corresponding to 50% (w/w) of alginate in **Figure 11**). In general, the incorporation of 10% (w/w) of MWCNTs did not affect the mechanical properties of Sepiolite/GNP/alginate bionanocomposites. The major difference observed in the MWCNTs doped bionanocomposites with respect to non-doped materials consists in a significant increase of the studied mechanical properties in the case of films containing 50% (w/w) of GNP. Finally, the bionanocomposite films containing the maximum amount of GNP, i.e. 55.6% (w/w) of GNP exhibit the highest values of the three studied parameters, attaining values in the same order of magnitude than those in the alginate films. In this case, the incorporation of 10% (w/w) MWCNTs does not influence significantly the mechanical

properties of the resulting composites. Water in the nanofillers is mainly associated with sepiolite as GNP only contains 0.3% (w/w) of water, which is physically adsorbed and can be easily eliminated at temperatures below 110 °C. In the final composite films, physically adsorbed water in sepiolite (e.g., sepiolite/GNP 2:1: 6.4% w/w, and sepiolite/GNP/MWCNT 2.5:1:0.1:6.1% w/w) can be reversibly eliminated without appreciable changes in the mechanical properties of the corresponding films.

As above indicated, the electrical conductivity of the prepared bionanocomposites have been measured in both perpendicular (*through-plane*) and parallel (*in-plane*) directions of the corresponding films with or without doping with carbon nanotubes (**Figure 12**). As expected, the *in-plane* electrical conductivity is much higher than *through-plane* conductivity, because the measurement is done on the surface of the film and the GNP conductive component has a tendency to lying parallel to the plane during the casting process. For the *through-plane* conductivity measurements, the film is compacted into a Swagelok cell and the current passing across the film. The observed anisotropy can be attributed to the lack of percolation in the perpendicular direction, the measured conductivity being then very low compared to the *in-plane* measurements. On the other hand, it is clearly observed that the presence of 10% (w/w) of MWCNTs with respect to the GNP content results in a significant increase of the electrical conductivity measured in both directions due to the role of carbon nanotubes affording elemental connections between particles in the composite increasing the percolation properties in these systems.

The bionanocomposite containing 55.6% (w/w) of GNP and 10% (w/w) of MWCNTs presents the best electrical conductivity. These results, together with those of the mechanical properties, indicate that the SEP:GNP:ALG:MWCNTs composite containing the higher amount of GNP, i.e. 55.6%, can be considered as the optimal material in the series here studied, showing the highest Young modulus, tensile strength and elongation at break, as well as and the highest electrical conductivity.

Other polymers with ability to form stable hydrogels such as gelatin and poly(vinyl alcohol) (PVA) were also studied by substituting alginate in the formulation, studying the sepiolite-GNP-polymer systems containing 55% (w/w) of GNP based on the results previously obtained for the alginate composites. The Raman spectra of diverse gelatin and PVA composites show the characteristic D and G bands of GNP, practically at the same frequencies than the ones observed for the pristine GNP, demonstrating scarce interaction of these nanoplatelets with the clay-bionanocomposite matrix (**Figure 10S**).^[46]

The results of mechanical properties (**Figure 13**) indicate that films based on alginate, present better mechanical properties, i.e. higher Young modulus, elongation at break and tensile strength, compared to those based on PVA and gelatin. Concerning the electrical conductivity (**Figure 14**) it can be remarked that the composites containing only GNP show a much lower conductivity compared to the systems containing also MWCNTs. In case of composites that only contain carbon nanotubes they present the highest electrical conductivity. Therefore, it is again observed that the incorporation of GNP is not sufficient to confer appreciable conductivity to the resulting nanocomposite films being necessary doping with carbon nanotubes to obtain films with appreciable conductivity. Comparing the electrical conductivity of the diverse films prepared from the different polymers here studied, it is observed that the films with alginate present the highest electrical conductivities compared to those prepared from gelatin and PVA (**Figure 11S**). It is clearly observed that, as expected, the higher conductivity values are obtained for materials containing MWCNTs, being reached conductivity values in the 50-2,500 S m⁻¹ range. These values are much higher than those reported for comparable systems prepared in absence of clays where reduced graphite oxide was incorporated in PVA leading to films showing four-probe conductivity values in the order of 10 S m⁻¹.^[47] The nature of the polymer matrix clearly affect to the electrical conductivity values of the composite films without any evident role of ionomer groups present in alginate and gelatin (eg. carboxylate in alginate). Incorporation of conducting polymers like PANI,

polypyrrole and PEDOT could be a valuable future approach to produce a significant increase of the conductivity in these clay/GNP/polymer composites taking into account the positive results obtained with polymer-clay nanocomposites incorporating conducting polymers as previously reported.^[18,48,49]

3. Conclusions

This work represents a first approach for the development of clay-composite systems involving graphene nanoplatelets. In the case of sepiolite, a fibrous clay of rheological grade, the application of sonomechanical treatments under optimized experimental conditions allows the generation of very stable dispersions of GNP, without any syneresis effect even after several months from their preparation. These dispersions lead to self-supported films of clay-GNP composites provided with reasonable electrical conductivity and mechanical properties. Electrical conductivity can be easily enhanced by doping with MWCNTs added during the GNP dispersion with the clay using sonomechanical treatments.

The textural behavior of sepiolite can be profited for adsorption of diverse species, as for instance organic dyes as here studied, but the interaction of the clay with diverse organic compounds or active metal and metal-oxide nanoparticles by anchoring to the silicate surface, may open the way for potential applications of these sepiolite–carbon functional materials that might find also interesting fields of use as membranes, heterogeneous catalysts, electrocatalysts and sensing devices among many other opportunities.

Also this work reports on the basis for obtaining functional nanocomposites based on the clay-GNP hybrids by assembly to diverse polymers, which can be conformed as films provided of tunable electrical conductivity and mechanical properties. It has been observed that the most favorable result corresponds to samples where alginate was added to the dispersion after ultrasonication in order to obtain stable dispersions. The *in-plane* conductivity is always higher than *through-plane* conductivity due to the tendency of graphene

nanoplatelets to lie flat due to their 2D crystal organization introducing a marked anisotropy to the resulting composite films. The presence of modest amounts of GNP is not enough to assure percolation to confer appreciable electrical conductivity to the nanocomposites. Doping with MWCNTs results in a significant increase of the electrical conductivity to values similar to the ones of films composed only by MWCNTs. In the most favorable case the composites can attain *in-plane* and *through-plane* electrical conductivity values of the order of 2500 and 0.05 S m⁻¹, respectively. In conclusion, small amounts of MWCNTs together with GNP-clay systems can be used as nanofillers in polymer-composites leading to significant electrical conductivity, maintaining the enhanced mechanical properties, at a lower cost which could be of great interest for diverse applications. In this context, Table 1S collects comparative properties of composite materials based on the present hydrogels assembled to the GNP-clay materials and other related systems reported in the bibliography, showing that the current GNP-clay composites can be useful as nanofillers in the preparation of conducting polymer composites.

4. Experimental Section

Materials

The natural magnesium silicate sepiolite here used was a rheological grade clay furnished by Tolsa S.A., under the commercial name PangelTM showing specific surface area (BET, N₂) of 344 m²/g and total pore volume of 0.577 cm³. Sodium-montmorillonite commercialized with cation exchange capacity (CEC) of *ca.* 90 mEq/100g, was supplied by Southern Clay Products Inc. (Gonzales, TX, USA) with the trade name of CloisiteTM-Na. Graphene nanoplatelets (abbreviated as GNP) are multilayered graphene sheets that were supplied by KNANOTM with the name of KNG-150. They are composed by more than ten carbon layers with 5-15 nm thickness and 1-20 μm diameter, showing conductivity of ~12,000 S m⁻¹ [36] and specific surface area of 41 m² g⁻¹ (from N₂ adsorption isotherms). GP500 Multilayered Graphene,

consisting of graphene platelets in a range of 5 to 10 layers, was supplied by Graphene-TechTM. According to the supplier, this sample shows specific surface area of ca. 500 m² g⁻¹, electrical conductivity of 650 S m⁻¹ (parallel to the surface) and 100 S m⁻¹ (perpendicular to the surface) and 40-300 nm lateral size of particles.^[50] CVD grown multiwalled carbon nanotubes (MWCNT) were obtained from Dropsens S.A. (Spain) being here used without further treatment. The tubes average diameter was 10 nm and the average length 1.5 µm. According to the supplier and in agreement to EDX analysis, the MWCNT consist on more than 95% carbon. The polysaccharide sodium alginate (ALG) (alginic acid sodium salt, from brown algae, with medium viscosity), poly(vinyl alcohol) (PVA) under the Mowiol® 20-98 trade name, MW ~125 kDa and gelatin (GEL) type A from porcine skin, were all acquired from Sigma Aldrich.

Preparation procedures

A) Clay-GNP samples

Water based montmorillonite- and sepiolite-GNP dispersions were prepared by adding ultra-pure water (R > 18.2 MX, Elga Maxima Ultra Pure Water system) (10 mL) to the appropriate amounts of clay and GNP (20 mg), followed by pulsed ultrasonic irradiation (US) (VC750 Sonics Vibra-Cell, operating at 20 kHz) using a 13 mm standard probe. Typically, they were carried out until an energy limit to 1 kJ using 10 s pulses separated by 10 s rest time (i.e. 10 s ON/10 s OFF). Then the suspensions were filtered under vacuum Millipore system with a hydrophilic membrane (MF-Millipore, VSWP04700, pore Ø = 25 nm). Self-supported composite films were easily peeled off from the membrane and dried overnight at 65 °C before characterization.

B) Sepiolite/GNP/MWCNT samples

Water based sepiolite/GNP/MWCNT dispersions were prepared by the same method described for sepiolite/GNP composites but incorporating MWCNT (2 mg) to the mixture at the same time than GNP.

C) *Sepiolite/GNP/MWCNT/polymer composites*

Alginate, gelatin and PVA composites were prepared by casting from solution of polymers using different proportions of sepiolite/GNP/MWCNT/polymer. Firstly, sepiolite and GNP/MWCNT components were dispersed in bidistilled water (5 mL) under US treatment under the same conditions than above reported for clay-GNP samples. Then, alginate, gelatin or PVA solutions (5 mL) were added while the systems were kept under magnetically stirring. The solutions of these biopolymers were prepared by slowly dissolving the respective polymer in water at room temperature in the case of alginate, at 50 °C for gelatin and 80 °C for PVA. The solutions were then cooled down at room temperature before being added to the suspensions of sepiolite and GNP/MWCNT. Each of the 10 mL dispersions were casted onto petri dish with Ø 90x14 mm (Deltalabs S.L.) and dried at 30°C with a control of relative humidity (60% RH) for 2 days using a CLIMACELL EVO Stability Chamber, Incubator model 111L.

Methylene blue adsorption

Methylene blue (MB) was used as model of cationic dye to evaluate the adsorption behavior of some graphene-clay materials. The materials were kept in a *ca.* $2 \cdot 10^{-5}$ M solution of MB in an orbital shaker operating at 160 min⁻¹ speed for 24 hours at room temperature. Once elapsed this time it is observed that the supernatant was completely clear with respect to the starting solution. The low dye concentration remaining in the supernatant was analyzed spectrophotometrically using a double beam UV–VIS spectrophotometer (Shimadzu, UV–1201 Spectrophotometer) by measuring the absorbance at 664 nm. The amount of adsorbed MB was also determined by CHNS chemical analysis performed in a LECO CHNS-932 instrument.

Characterization

X-ray diffraction (XRD) data were collected on film samples using a BRUKER D8-ADVANCE diffractometer working at 40 kV and 30 mA and using Ni-filtered Cu K α

radiation, with a scan step of 2°/min between 2θ values of 2 and 70°. Infrared spectra (IR) were obtained using an Attenuated Total Reflectance (ATR) equipment (Shimadzu, IRAffinity-1, GladiATR10). Fourier transform infrared (FTIR) spectra were recorded with a FTIR spectrometer BRUKER IFS 66V-S. Each sample was placed in the sample holder as KBr pellets (2% wt sample concentration pelletized at 10 Ton) and scanned from 4000 to 400 cm^{-1} with 2 cm^{-1} resolution. The amount of carbon content in the sepiolite-GNP or sepiolite-GNP-MWCNT samples were determined by CHN elemental chemical microanalysis in a LECO-CHNS-932 analyzer. The thermal behavior of some prepared samples was analyzed from the simultaneously recorded thermogravimetric (TG) and differential thermal analysis (DTA) curves in a SEIKO SSC/5200 equipment, in experiments carried out under nitrogen atmosphere (flux of 100 ml/min) from room temperature to 1000 °C at 10 °C min^{-1} heating rate. Raman spectra were obtained using a 532 nm laser (μ Sense-LabC1X Enwave Optronics Raman Confocal equipment). The viscosity measurements were carried out in a RVDVII+ Pro Brookfield viscometer operating at 20-22 °C. The specific surface area and the porosity of the samples were determined from N_2 adsorption/desorption isotherms at -196 °C using a static volumetric apparatus, Micromeritics ASAP 2010 analyzer. The samples (150–200 mg) were outgassed, previously to the analysis, at 120 °C until the pressure remains constant and less than 0.005 Torr. The BET specific surface area was calculated from the nitrogen adsorption data in the relative pressure range from 0.05 to 0.3. The external surface area and micropore volume was obtained by means of the t -plot according to De Boer's method. The total pore volume (V_T) was estimated from the amount of nitrogen adsorbed at relative pressure $P/P^0 = 0.96$ in the desorption branch of the isotherm, which was also used to calculate the pore size distributions.^[35,51,52] For certain samples the specific surface area was estimated using the so-called “single-point” method, using a Micromeritics FLOWSORB 2300 model equipment.

Field-emission scanning electron microscopy was performed with a FE-SEM equipment FEI-NOVA NanoSEM 230, which allows direct observation of the samples adhered on a carbon tap without requirement of any conductive coating on the surface samples. Energy dispersive X-ray analysis (EDX) was determined with an EDAX detector type Apollo 10 SDD mounted on the FE-SEM equipment. The electrical conductivity was measured using two distinct equipments, one measuring the *in-plane* electrical conductivity and other one measuring the perpendicular conductivity (*through-plane*) of the formed films. For the in-plane conductivity measurements, it was used an in-line four probe configuration using a multichannel potentiostat (Solartron Multistat 1480) operating in galvanodynamic mode. Four voltage-currents were applied for each film using a frequency response analyser (Solartron 1260) to analyze the impedance of samples by applying 300 mA amplitude signal over the frequency range of 10^2 to 10^6 Hz. The resistance average values were calculated for each sample and the resistivity was determined based on the setup and geometrical configuration of the samples. The perpendicular conductivity was measured using a homemade electrochemical cell based on a Swagelok® device with a Teflon™ body and stainless steel current collectors, using a digital multimeter. The film thickness was measured with a high-accuracy Mitutoyo Outside 2118-50/7053 Micrometer device.

Stress-strain curves were obtained with an INSTRON 3345 model Universal Testing Machine (Instron Corp., Canton, MA, USA). The film samples were cut with a rectangular shape (*ca.* 10 mm x 30 mm) and mounted between appropriated grips with an initial separation of 20 mm, the cross-head speed being set at $5 \text{ mm} \cdot \text{min}^{-1}$. Three replicates were run for each sample. The elongation was directly determined from the crosshead displacement as the machine was not equipped with an extensometer. Tensile modulus (E), percentage of elongation at break (E_b) and elastic modulus (or Young's modulus) of films were calculated using the Instron software.

Supporting Information

Supporting Information is available from the Wiley Online Library or from the author.

Acknowledgements

This work was partially supported by the MINECO, Spain (Project MAT2012-31759 and MAT2015-71117-R) and FCT/MEC, Portugal (CICECO-Aveiro Institute of Materials - POCI-01-0145-FEDER-007679, FCT UID/CTM/50011/2013), through national funds and where applicable co-financed by the FEDER, within the PT2020 Partnership Agreement. EU COST Action MP1202 is also acknowledged. C. Nunes and P. Ferreira thank FCT for their grants SFRH/BPD/100627/2014 and IF/00327/2013, respectively.

The authors thank Dr. M. Darder for fruitful discussions, Mr. A. Valera for imaging samples under the FE-SEM, and Mr. R. Barrios for N₂ adsorption measurements. We are gratefully acknowledged to Xiamen Knano Graphene Technology Co. and GRAPHENE-TECH companies for giving us KNG-150 graphene nanoplatelets and GP 500 Multilayered Graphene samples, respectively.

Received: ((will be filled in by the editorial staff))

Revised: ((will be filled in by the editorial staff))

Published online: ((will be filled in by the editorial staff))

- [1] K. S. Novoselov, A. K. Geim, S. V. Morozov, D. Jiang, Y. Zhang, S. V. Dubonos, I. V. Grigorieva, A. A. Firsov, *Science* **2004**, *306*, 666.
- [2] a) Y. Zhu, S. Murali, W. Cai, X. Li, J. W. Suk, J. R. Potts, R. S. Ruoff, *Adv. Mater.* **2010**, *22*, 3906; b) V. Singh, D. Joung, L. Zhai, S. Das, S. I. Khondaker, S. Seal, *Prog. Mater. Sci.* **2011**, *56*, 1178; c) M. Terrones, A. R. Botello-Mendez, J. Campos-Delgado, F. Lopez-Urias, Y. I. Vega-Cantu, F. J. Rodriguez-Macias, A. L. Elias, E. Munoz-Sandoval, A. G. Cano-Marquez, J.-C. Charlier, H. Terrones, *Nano Today* **2010**, *5*, 351; d) X. Huang, X. Qi, F. Boey, H. Zhang, *Chem. Soc. Rev.* **2012**, *41*, 666; e) R. M. Frazier, D. T. Daly, R. P. Swatloski, K. W. Hathcock, C. R. South, *Recent Pat. Nanotechnol.* **2009**, *3*, 164; f) L. Ruitao, J. A. Robinson, R. E. Schaak, S. Du, S. Yifan, T. E. Mallouk, M. Terrones, *Acc. Chem. Res.* **2015**, *48*, 56.
- [3] F. Bergaya, G. Lagaly, in *Developments in Clay Science, Vol. 5* (Eds: B. Faïza, L. Gerhard), Elsevier, **2013**, Ch. 1.
- [4] https://en.wikipedia.org/wiki/Pencil#Discovery_of_graphite_and_clay_mixing, April, 2016.
- [5] <https://web.archive.org/web/20090619105057/http://www.pencils.co.uk/products/derwent.aspx?sid=3&p=1>, April, 2016.
- [6] a) T. Kyotani, N. Sonobe, A. Tomita, *Nature* **1988**, *331*, 331; b) Z. X. Ma, T. Kyotani, A. Tomita, *Chem. Commun.* **2000**, 2365; c) Z. X. Ma, T. Kyotani, Z. Liu, O. Terasaki, A. Tomita, *Chem. Mater.* **2001**, *13*, 4413.
- [7] R. Fernandez-Saavedra, P. Aranda, E. Ruiz-Hitzky, *Adv. Funct. Mater.* **2004**, *14*, 77.
- [8] a) T. J. Bandoz, J. Jagiello, K. Putyera, J. A. Schwarz, *Chem. Mater.* **1996**, *8*, 2023; b) G. Sandi, R. E. Winans, K. A. Carrado, *J. Electrochem. Soc.* **1996**, *143*, L95; c) T. J. Bandoz, J. Jagiello, K. Putyera, J. A. Schwarz, *Chemistry of Materials Chem. Mater.* **1996**, *8*, 2023; d) L. Duclaux, E. Frackowiak, T. Gibinski, R. Benoit, F. Beguin, *Mol. Cryst. Liq. Cryst.* **2000**, *340*, 449; e) G. Sandi, K. A. Carrado, H. Joachin, W. Lu, J. Prakash, *J. Power Sources* **2003**, *119*, 492; f) A. Bakandritsos, T. Steriotis, D. Petridis, *Chem. Mater.* **2004**, *16*, 1551; g) F. Leroux, M. Dubois, *J. Mater. Chem.* **2006**, *16*, 4510; h) V. Malgras, Q. Ji, Y. Kamachi, T. Mori, F. Shieh, *Bull. Chem. Soc. Jpn.* **2015**, *88*, 1171.
- Kevin C.-W. Wu, Katsuhiko Ariga,*1 and Yusuke Yamauchi
- [9] P. Aranda, in *CMS Workshop Lectures Series*, Vol. 15 (Eds: K. A. Carrado, F. Bergaya), The Clay Minerals Society, Chantilly, VA, **2007**.
- [10] P. Aranda, M. Darder, R. Fernandez-Saavedra, M. Lopez-Blanco, E. Ruiz-Hitzky, *Thin Solid Films* **2006**, *495*, 104.
- [11] A. Gomez-Aviles, M. Darder, P. Aranda, E. Ruiz-Hitzky, *Angew. Chem., Int. Ed.* **2007**, *46*, 923.
- [12] A. Gomez-Aviles, M. Darder, P. Aranda, E. Ruiz-Hitzky, *Appl. Clay Sci.* **2010**, *47*, 203.
- [13] R. Fernandez-Saavedra, M. Darder, A. Gomez-Aviles, P. Aranda, E. Ruiz-Hitzky, *J. Nanosci. Nanotechnol.* **2008**, *8*, 1741.
- [14] C. Xu, G. Ning, X. Zhu, G. Wang, X. Liu, J. Gao, Q. Zhang, W. Qian, F. Wei, *Carbon* **2013**, *62*, 213.
- [15] E. Ruiz-Hitzky, M. Darder, F. M. Fernandes, E. Zatile, F. J. Palomares, P. Aranda, *Adv. Mater.* **2011**, *23*, 5250.

- [16] C. Ruiz-Garcia, J. Perez-Carvajal, A. Berenguer-Murcia, M. Darder, P. Aranda, D. Cazorla-Amoros, E. Ruiz-Hitzky, *Phys. Chem. Chem. Phys.* **2013**, *15*, 18635.
- [17] C. Ruiz-Garcia, M. Darder, P. Aranda, E. Ruiz-Hitzky, *J. Mater. Chem. A* **2014**, *2*, 2009.
- [18] E. Ruiz-Hitzky, M. Darder, F. M. Fernandes, B. Wicklein, A. C. S. Alcantara, P. Aranda, *Prog. Polym. Sci.* **2013**, *38*, 1392.
- [19] E. Ruiz-Hitzky, P. Aranda, A. Álvarez, J. Santarén, A. Esteban-Cubillo, in *Developments in Clay Science*, Vol. 3 (Eds: E. Galán, S. Arie), Elsevier, **2011**, Ch.17.
- [20] K. Brauner, A. Preisinger, *Tschermaks Mineral. Petrogr. Mitt.* **1956**, *6*, 120.
- [21] J. Santaren, J. Sanz, E. Ruiz-Hitzky, *Clays Clay Miner.* **1990**, *38*, 63.
- [22] E. Ruiz-Hitzky, *J. Mater. Chem.* **2001**, *11*, 86.
- [23] C. Zhang, W. W. Tjiu, W. Fan, Z. Yang, S. Huang, T. Liu, *J. Mater. Chem.* **2011**, *21*, 18011.
- [24] W. S. Hummers, R. E. Offeman, *J. Am. Chem. Soc.* **1958**, *80*, 1339.
- [25] D. K. Chouhan, T. U. Patro, G. Harikrishnan, S. Kumar, S. Gupta, G. S. Kumar, H. Cohen, H. D. Wagner, *Appl. Clay Sci.* <http://dx.doi.org/10.1016/j.clay.2016.05.023>
- [26] X. Diez-Betriu, S. Alvarez-Garcia, C. Botas, P. Alvarez, J. Sanchez-Marcos, C. Prieto, R. Menendez, A. de Andres, *J. Mater. Chem. C* **2013**, *1*, 6905.
- [27] Y. Liu, X. Jiang, B. Li, X. Zhang, T. Liu, X. Yan, J. Ding, Q. Cai, J. Zhang, *J. Mater. Chem. A* **2014**, *2*, 4264.
- [28] M. Safaei, A. Sheidaei, M. Baniassadi, S. Ahzi, M. M. Mashhadi, F. Pourboghra, *Comput. Mater. Sci.* **2015**, *96*, 191.
- [29] S. Paszkiewicz, I. Pawelec, A. Szymczyk, Z. Roslaniec, *Pol. J. Chem. Technol.* **2015**, *17*, 74.
- [30] H. Fukushima, L. T Drzal, B. P. Rook, M. J. Rich, *J. Therm. Anal. Calorim.* **2006**, *85*, 235.
- [31] D. Zhuo, R. Wang, L. Wu, Y. Guo, L. Ma, Z. Weng, J. Qi, *J. Nanomater.* **2013**, *83*, 1.
- [32] F. M. Fernandes, E. Ruiz-Hitzky, *Carbon* **2014**, *72*, 296
- [33] L. Bokobza, J.L. Bruneel, M. Couzi, *Vib. Spectrosc.* **2014**, *74*, 57.
- [34] J. Y. Lee, I. In, *Chem. Lett.* **2011**, *40*, 567.
- [35] F. Rouquerol, J. Rouquerol, K. Sing, in *Adsorption by Powders and Porous Solids*, Academic Press, London, **1999**.
- [36] <http://www.knano.com.cn/En/product.aspx?IntroCateID=1667&CateID=1667>, June, 2016.
- [37] A. J. Aznar, B. Casal, E. Ruiz-Hitzky, I. Lopez-Arbeloa, F. Lopez-Arbeloa, J. Santaren, A. Alvarez, *Clay Miner.* **1992**, *27*, 101.
- [38] H. Van Olphe., *Science* **1966**, *154*, 645.
- [49] M. S. Del Rio, P. Martinetto, C. Reyes-Valerio, E. Dooryhee, M. Suarez, *Archaeometry* **2006**, *48*, 115.
- [40] C. Ouellet-Plamondon, P. Aranda, A. Favier, G. Habert, H. Van Damme, E. Ruiz-Hitzky, *RSC Adv.* **2015**, *5*, 98834.
- [41] E. Ruiz-Hitzky, P. Aranda, M. Darder, in *Kirk-Othmer Encyclopedia of Chemical Technology*, John Wiley & Sons, Inc., **2000**.
- [42] E. Ruiz-Hitzky, M. Darder, P. Aranda, in *Bio-inorganic Hybrid Nanomaterials: Strategies, Syntheses, Characterization and Applications*, (Eds: E. Ruiz-Hitzky, K. Ariga, Y. M. Lvov), Wiley-VCH Verlag GmbH & Co. KGaA, **2008**, Ch.1.
- [43] M. Darder, P. Aranda, E. Ruiz-Hitzky, *Adv. Mater.* **2007**, *19*, 1309.
- [44] E. Ruiz-Hitzky, M. Darder, P. Aranda, K. Ariga, *Adv. Mater.* **2010**, *22*, 323.
- [45] A. C. S. Alcantara, M. Darder, P. Aranda, S. Tateyama, M. K. Okajima, T. Kaneko, M. Ogawa, E. Ruiz-Hitzky, *J. Mater. Chem. A* **2014**, *2*, 1391.
- [46] M. Goumri, J. W. Venturini, A. Bakour, M. Khenfouch, M. Baitoul, *Appl. Phys. A* **2016**, *122*, 212.
- [47] H. J. Salavagione, G. Martinez, M. A. Gomez, *J. Mater. Chem.* **2009**, *19*, 5027.
- [48] S. Letaief, P. Aranda, E. Ruiz-Hitzky, *Appl. Clay Sci.* **2005**, *28*, 183.
- [49] E. Ruiz-hitzky, *Adv. Mater.* **1993**, *5*, 334.
- [50] http://graphene-tech.net/Fichas_tecnicas_2014/GP500_Technical_Data_Sheet.pdf, June, 2016.
- [51] B. C. Lippens, J. H. Deboer, *J. Catal.* **1965**, *4*, 319.
- [52] C. Wang, L. Juang, C. Lee, T. Hsu, J. Lee, H. Chao, *J. Colloid Interface Sci.* **2004**, *280*, 27.

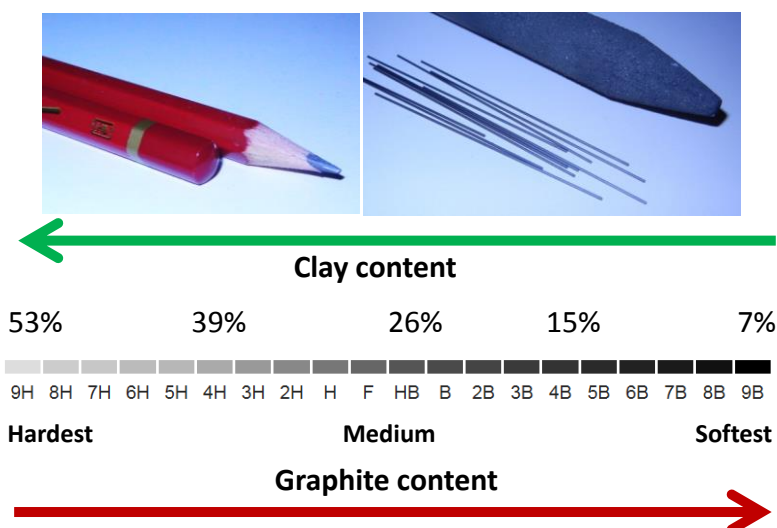


Figure 1. Graphite-clay composite currently used as core of pencils (pencil leads). The content in clay corresponds to the tone of pencils, in this example from 9H (hardest) to 9B (softest).

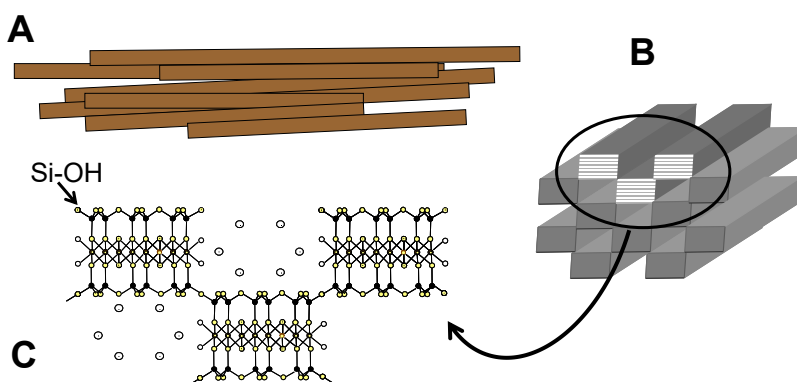


Figure 2. Scheme of sepiolite fibers arranged as bundles (A), ideal cross-section of a single fiber (B), and crystal structure with alternating blocks of magnesium silicate and tunnels (C). Location of silanol groups of the silicate at the external surface of fibers are also indicated in C.

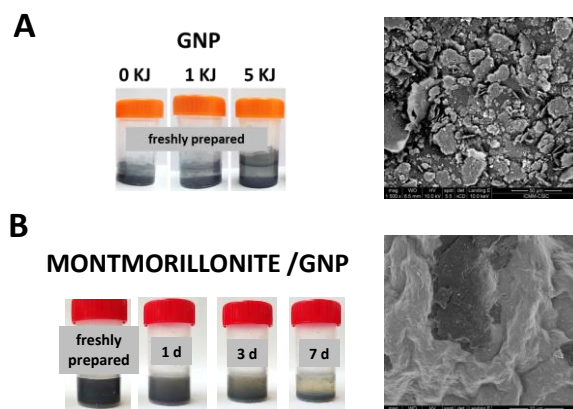


Figure 3. Aspect of water dispersions of A) GNP dispersed in water submitted to 1 kJ and 5 kJ of ultrasound irradiation energy, and B) dispersions of montmorillonite/GNP of 2.5:1 (w/w) composition by ultrasound irradiation with 1 kJ of total energy after 1, 3 and 7 days of stand. The pictures on the right part correspond to FE-SEM images of representative examples of the dried dispersions on the left.

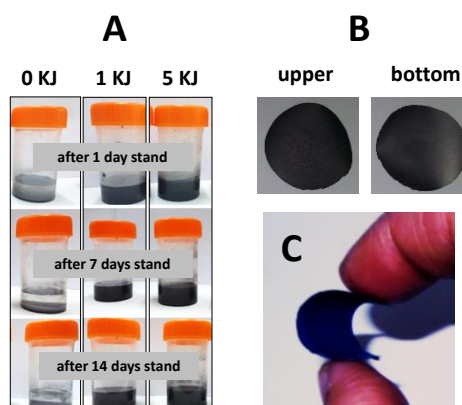


Figure 4. Sepiolite/GNP composites: A) Aspect after 1, 7 and 14 days of stand of 2.5:1 (w/w) sepiolite/GNP water dispersions without (0 kJ) and submitted to 1 kJ and 5 kJ of US energy irradiation; B) Self-supported film obtained by vacuum filtration of 0.5:1 (w/w) sepiolite/GNP water dispersion showing the both, upper and bottom, surfaces. The flexibility of these films is shown in C.

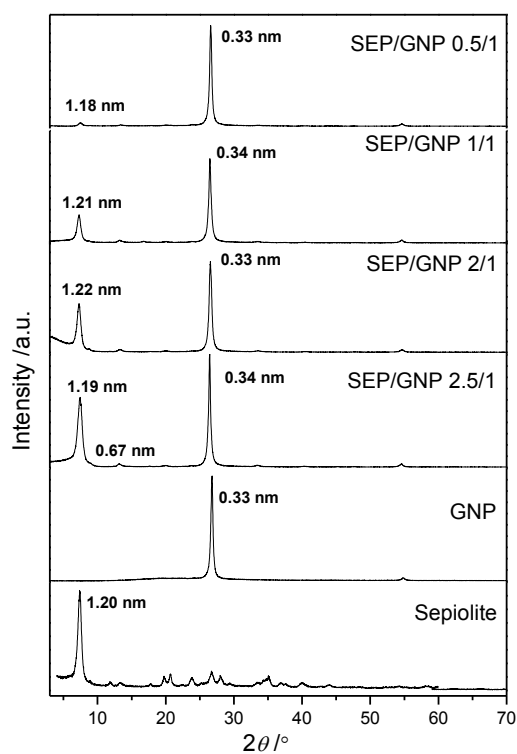


Figure 5. XRD patterns of starting sepiolite (SEP) and graphene nanoplatelets (GNP) components and the resulting composites prepared as self-supported films with different clay/GNP (w/w) proportions, from 2.5/1 to 0.5/1 (from down to top).

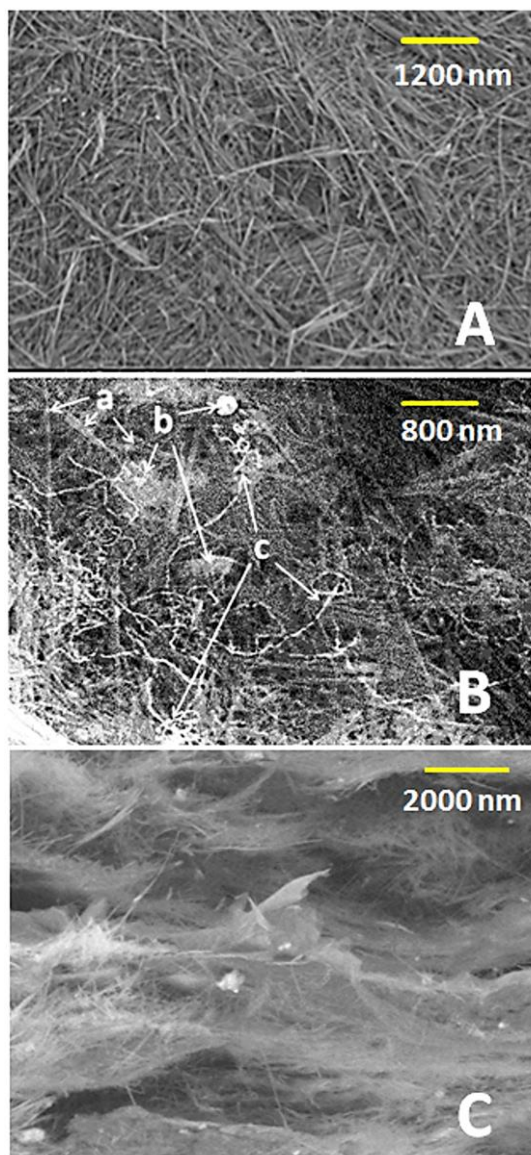


Figure 6. FE-SEM images of samples A) SEP/GNP 10:1; B) SEP/GNP/MWCNTs 2.5:1:0.1 (arrows indicate the presence of a: sepiolite fibers, b: GNP, c: MWCNTs); and C) cross-section of SEP/GNP/MWCNTs 0.5:1:0.1 film.

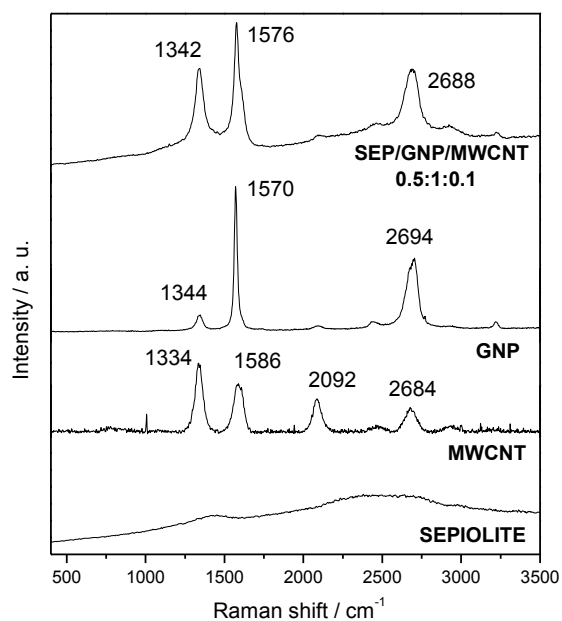


Figure 7. Comparison of Raman spectra of sepiolite, MWCNT, GNP, and sepiolite/GNP 0.5:1 (w/w) composite (doped with MWCNTs).

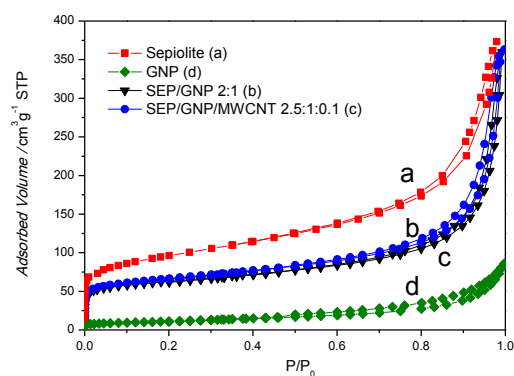


Figure 8. N_2 adsorption-desorption isotherms (77 K) of sepiolite (a) and GNP (d) components, and of sepiolite/GNP 2:1 (w/w) and sepiolite/GNP/MWCNTs 2.5:1:0.1 (w/w) composites, (c) and (b) respectively.

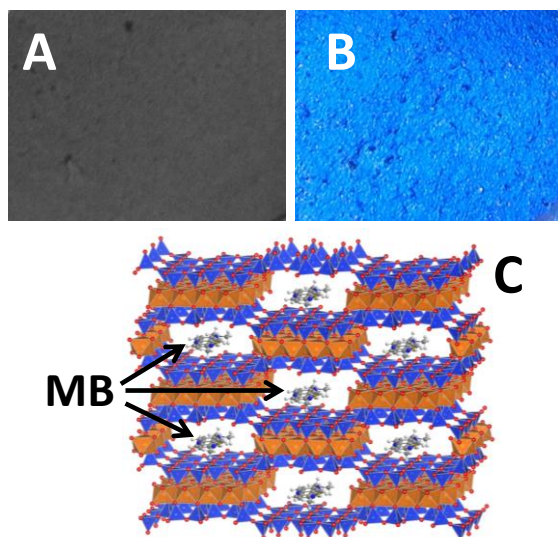


Figure 9. Sepiolite/GNP/MWCNTs self-supported film (A) after treatment with methylene blue (MB) molecular dye giving rise to clay-carbon colored material (B), where MB remain entrapped into the silicate cavities as represented in the sepiolite structure (C).

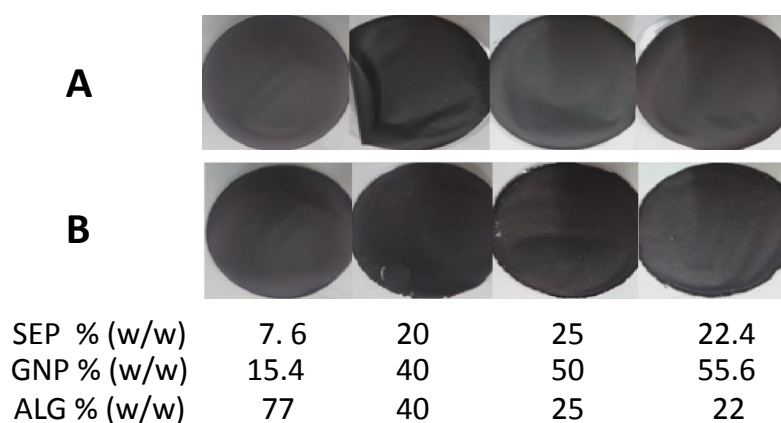


Figure 10. Bionanocomposite films of A) SEP/GNP/ALG with variable GNP content (% w/w) and B) SEP/GNP/MWCNTs/ALG containing 10% (w/w) of MWCNTs in the resulting composites.

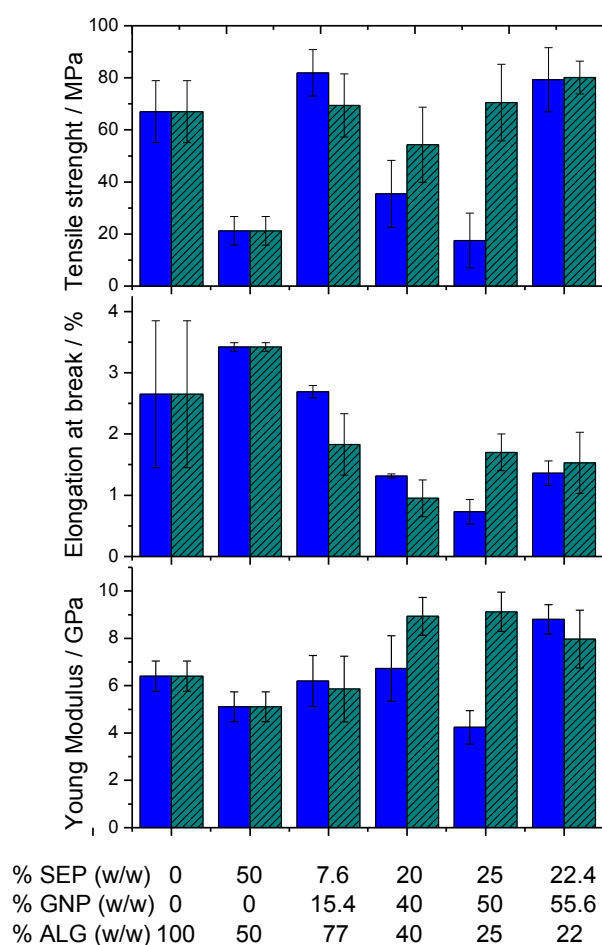


Figure 11. Mechanical properties of self-supported films of sepiolite (SEP)/GNP/alginate (ALG) nanocomposites (left bars) with different proportions of the involved components, and MWCNTs doped systems (right bars) incorporating 10% (w/w) of carbon nanotubes with respect to the GNP content

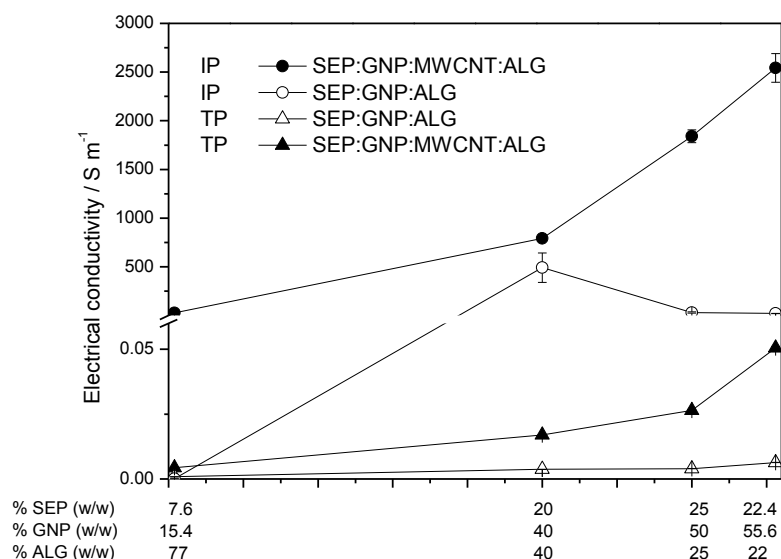


Figure 12. *In-plane (IP)* and *through-plane (TP)* electrical conductivity of films of sepiolite, GNP and alginate-based bionanocomposites without and with MWCNTs doping (10% w/w MWCNTs with respect to the GNP content).

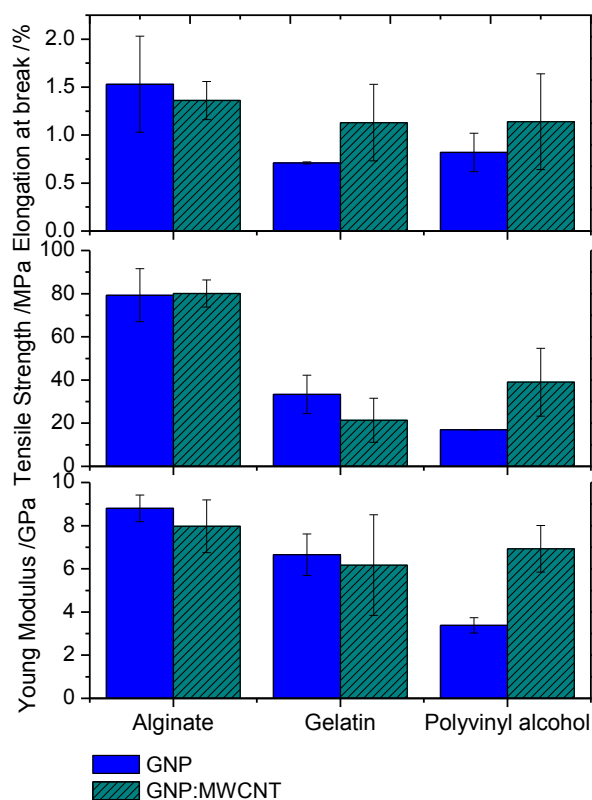


Figure 13. Mechanical properties of sepiolite/GNP/polymer composites containing 55% (w/w) of GNP, without and with addition of 10% (w/w) of MWCNT in relation to GNP content.

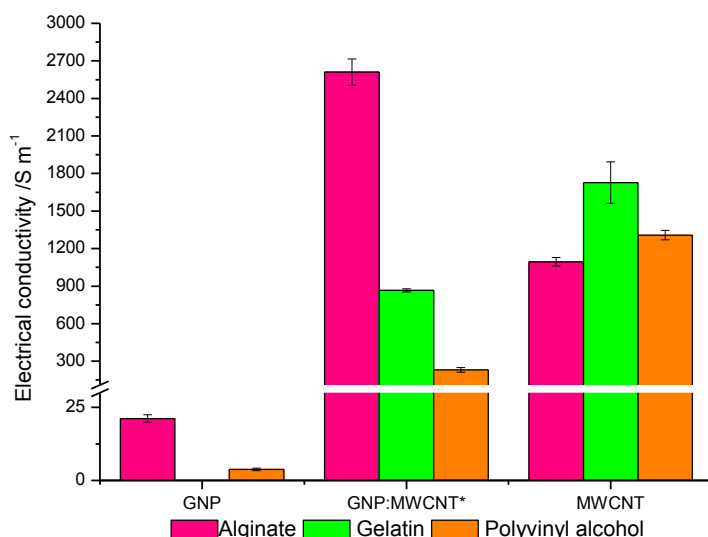


Figure 14. *In-plane* electrical conductivity of sepiolite/GNP/polymer, and sepiolite/GNP/MWCNTs/polymer and sepiolite/MWCNTs/polymer composite films prepared from diverse polymers (alginate, gelatin and polyvinyl alcohol).

Table 1. Characteristics of clay-carbon composite films made of sepiolite assembled to GNP and GNP/MWCNTs with different initial composition.

Initial components (w/w)			Resulting composites			
Sepiolite	GNP	MWCNTs	C (%)*	S_0 (m ² g ⁻¹)	σ^\dagger (S m ⁻¹)	σ^\equiv (S m ⁻¹)
10.0	1	-	9.3 (9.1)	263	<0.10	-
5.0	1	-	17.1 (16.7)	213	<0.10	-
2.5	1	-	25.8 (28.6)	185	<0.10	-
2.0	1	-	31.1 (33.3)	186**	<0.10	n.d.
1.5	1	-	38.2 (40.0)	151	<0.10	-
1.0	1	-	46.3 (50.0)	164	<0.10	n.d.
0.5	1	-	62.7 (66.7)	95	0.12	3.5
2.5	1	0.1	27.7 (27.7)	207**	0.13	75.5
0.5	1	0.1	64.0 (62.5)	145	0.19	2633

* values in parentheses indicate the theoretical percentage of carbon; S_0 : specific surface area estimated from the “single point” method, except when deduced from N₂ adsorption-desorption isotherms using BET theory (**); electrical conductivity was measured *through-plane* (σ^\dagger) or *in-plane* (σ^\equiv) direction to the composite film plane; n.d.: not detected.

Table 2. Textural characteristics of the starting components, sepiolite (from Vallecas-Vicálvaro, Spain) and graphene nanoplatelets (KNG150), the resulting sepiolite/GNP composite in 2:1 w/w ratio, and the composite doped with carbon nanotubes (sepiolite/GNP/MWCNT in 2.5:1:0.1 w/w ratio).

Sample	S_{BET} ($\text{m}^2 \text{g}^{-1}$)	S_{EXT} ($\text{m}^2 \text{g}^{-1}$)	$S_{\text{MICROP.}}$ ($\text{m}^2 \text{g}^{-1}$)	$V_{\text{MICROP.}}$ ($\text{cm}^3 \text{g}^{-1}$)	V_{TOTAL} ($\text{cm}^3 \text{g}^{-1}$)
sepiolite (Pangel TM)	344	221	123	0.052	0.577
graphene-nanoplatelets (GNP-KNG150)	41	39.7	1.3	0.0004	0.125
sepiolite/GNP (2:1)	186	112	74	0.048	0.470
sepiolite/GNP/MWCNT (2.5:1:0.1)	207	123	84	0.049	0.537

S_{BET} : specific surface area from the adsorption-desorption N_2 isotherms (77 K); S_{EXT} : external surface; $S_{\text{MICROP.}}$: micropores surface; $V_{\text{MICROP.}}$: micropore volume; V_{TOTAL} : total pore volume.

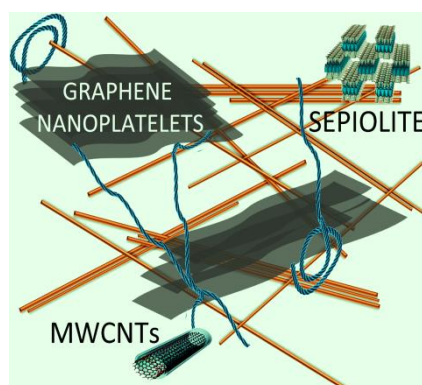
Table of contents entry:

Graphene-based composites are prepared by assembling graphene nanoplatelets to clay minerals using sonomechanical treatment. Sepiolite fibrous clay produces very stable water dispersions even for low clay content giving rise to homogenous composites at the nano/microscale. The process allows incorporation of other components such as MWCNTs, molecular dyes and polymers, giving rise to functional materials showing enhanced electrical conductivity and other predesigned properties.

Keywords: clay, graphene, graphite, composite, biopolymer

E. Ruiz-Hitzky*, M.C.C. Sobral, A. Gómez-Avilés, C. Nunes, C. Ruiz-García, P. Ferreira, P. Aranda

Clay-graphene nanoplatelets functional **conducting** composites

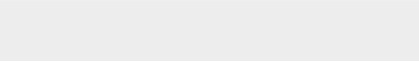
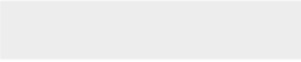




[Click here to access/download](#)

Supporting Information

E. Ruiz-Hitzky et al. Supporting information_revised
version.docx





[Click here to access/download](#)

Production Data

E.RUIZ-HITZKY et al. revised manuscript.docx

